Title

Multitarget molecule, PTUPB, to treat diabetic nephropathy in rats

Journal

British Journal of Pharmacology, 178(22)

ISSN

0007-1188

Authors

Khan, Abdul Hye

Hwang, Sung Hee

Barnett, Scott D

et al.

Publication Date

2021-11-01

DOI

10.1111/bph.15623

Peer reviewed

HHS Public Access

Author manuscript

Br J Pharmacol. Author manuscript; available in PMC 2022 November 01.

Published in final edited form as:

Br J Pharmacol. 2021 November ; 178(22): 4468–4484. doi:10.1111/bph.15623.

MULTI-TARGET MOLECULE TO TREAT DIABETIC NEPHROPATHY IN RATS

Md. Abdul Hye Khan[1,*], **Sung Hee Hwang**[4], **Scott D. Barnett**[1], **Anna Burkhan**[1], **Wojciech K. Jankiewicz**[1], **Bruce D. Hammock**[4], **John D. Imig**[1,*]

[1]Drug Discovery Center and Cardiovascular Center, Medical College of Wisconsin, Milwaukee, WI 53226, USA

[4]Department of Entomology and Nematology and Comprehensive Cancer Center, University of California, Davis, CA 95616, USA

Abstract

Diabetic nephropathy is one of the most common complications that is related to high morbidity and mortality in type 2 diabetic patients. We investigated ability of a novel dual modulator, PTUPB that concurrently acts as a soluble epoxide hydrolase inhibitor and as a cyclooxygenase-2 inhibitor against diabetic nephropathy. Sixteen week-old type 2 diabetic and proteinuric obese ZSF1 rats were treated with vehicle, PTUPB, or enalapril for 8 weeks. Obese ZSF1 rats were diabetic with 5-fold higher fasting blood glucose levels and markedly higher HbA1c levels compared to lean ZSF1 rats. Neither PTUPB nor enalapril reduced fasting blood glucose or HbA1c in obese ZSF1 rats. The obese ZSF1 rats also developed diabetic nephropathy with elevated albuminuria and tubular and glomerular injuries. PTUPB alleviated diabetic nephropathy in obese ZSF1 rats by reducing albuminuria by 50%, renal cortical and medullary cast formation by 60–70%, renal fibrosis by 40–50%, and glomerular injury by 55%. In PTUPB treated obese ZSF1 rats, glomerular nephrin expression was preserved. Enalapril treatment demonstrated an effect comparable to PTUPB and alleviated diabetic nephropathy in obese ZSF1 rats by reducing all kidney injury parameters by 30 to 50%. Diabetic renal injury in obese ZSF1 rats was accompanied by renal inflammation with 6–7fold higher urinary MCP-1 level and renal infiltration of CD-68 positive cells. PTUPB and enalapril treatment reduced renal inflammation with significantly reduced urinary MCP-1 levels and renal mRNA expression of cytokines. PTUPB demonstrated superior anti-inflammatory actions compared to enalapril treatment. Obese ZSF1 rats were also hypertensive, hyperlipidemic, and exhibited liver injury. Both PTUPB and enalapril lowered blood pressure in obese ZSF1 rats. Interestingly, PTUPB but not enalapril decreased hyperlipidemia and liver injury in Obese ZSF1 rats. Overall, we demonstrate that a dual modulator PTUPB does not treat hyperglycemia, but can effectively alleviate hypertension, diabetic nephropathy, hyperlipidemia and liver injury in type 2 diabetic rats. Our data further

[*]Corresponding authors: John D. Imig, PhD, Md Abdul Hye Khan, PhD, Drug Discovery Center, Medical College of Wisconsin, 8701 Watertown Plank Road, Milwaukee, Wisconsin 53226, USA, jdimig@mcw.edu, abhkhan@mcw.edu.

DISCLOSURE

The dual inhibitor is covered under a University of California Patent with Sung Hee Hwang and Bruce D. Hammock. Other authors declare no conflicts of interest, financial or otherwise.

demonstrate that the renal actions of PTUPB is comparable to a current standard diabetic nephropathy treatment.

Keywords

type 2 diabetes; diabetic nephropathy; soluble epoxide hydrolase; cyclooxygenase; multi-target drugs

INTRODUCTION

Diabetes is a significant health problem worldwide. Globally 8.5% of adults aged 18 years and older have diabetes and diabetes was the direct cause of 1.6 million deaths in 2016. The high mortality and morbidity associated with diabetes is due to several complications. One of the most common diabetic complications is micro- and macro-vascular dysfunction that results in diabetic nephropathy that progresses to end-stage renal diseases (ESRD) and death (Li et al., 2010; Bugger and Abel, 2014). Approximately 20–40% of diabetic patients develop nephropathy, and due to the growing incidence of diabetes, diabetic nephropathy is now the main cause of ESRD worldwide (Tesch, 2015; Toth-Manikowski and Atta, 2015). Moreover, diabetic nephropathy incidence rates show no signs of slowing. In the USA alone, 42% of all ESRD cases had a diagnosis of diabetic nephropathy (Warren et al., 2019).

Besides glycemic control with anti-diabetic drugs, renin angiotensin system (RAS) blockers have been the standard of care to treat diabetic nephropathy. Unfortunately, approximately one-half of diabetic patients fail to achieve acceptable glycemic control with the currently available anti-diabetic options and RAS blockers have been mildly effective in reducing diabetic nephropathy progression to ESRD. Consequently, morbidity and mortality associated with diabetes is still high because of complications such as hypertension and diabetic nephropathy (Stark et al., 2013). The poor treatment outcome with the present anti-diabetic drugs is also partly due to uncontrolled comorbid risk factors such as dyslipidemia in type 2 diabetes (Stark et al., 2013). Indeed, according to the American Diabetic Association, during the period of 2009–2012 about 65–70% of diabetic patients had pre-existing dyslipidemia and other complications at the time of diagnosis (Afkarian et al., 2013; Magee et al., 2017). Thus, there is an urgent need for novel treatments that reduce cardiovascular risk and have a favorable impact on comorbid conditions such as diabetic nephropathy.

With this background, the present study investigated the ability of a novel dual acting molecule soluble epoxide hydrolase (sEH) and cyclooxygenase-2 (COX-2) inhibitor, PTUPB, to treat diabetic nephropathy in obese ZSF1 rats. The obese ZSF1 rat is widely used as a model of type 2 diabetes with associated nephropathy and comorbid conditions that are often present in type 2 diabetic human patients. Our findings demonstrate promising potential for PTUPB to treat diabetic nephropathy by acting on multiple pathophysiological components.

MATERIALS AND METHODS

Chemicals

The chemistry and synthesis process for the dual sEH and COX-2 inhibitor PTUPB [(4-(5-phenyl-3-{3-[3-(4-trifluoromethylphenyl)-ureido]-propyl}-pyrazol-1-yl)-benzenesulfonamide),] is described previously (Hwang et al., 2011). All chemicals used in this study were purchased from Sigma Aldrich (St Louis, MO, USA) unless otherwise mentioned.

Animal studies

All experiments are approved (protocol numbers AUA00001818, 9/5/2019 and AUA00000042, 10/11/2019) by the Medical College of Wisconsin Institutional Animal Care and Use Committee that concurs with the National Institutes of Health Guidelines. In the Biomedical Resource Center at the Medical College of Wisconsin the rats were housed with a 12/12h light–dark cycle with free access to water and rat chow. All animals were acclimatized for 7 days before they were used in any experimental protocol. All studies were designed to generate groups of equal size, using randomisation and blinded analysis.

Experimental design

These studies were carried out in 16 week-old, male obese ZSF1 rats (ZSF1-Lepr^{fa}Lepr^{cp}/Crl; strain code 378) and lean ZSF1 rats (strain code 379) obtained from Charles River Laboratories. The ZSF1 rat is a cross between Zucker Diabetic Fatty (ZDF) female and Spontaneously Hypertensive Heart Failure (SHHF) male rats. These rats are known to be an excellent model of diabetic nephropathy (Bilan et al., 2011; Su et al., 2016).

As we have described in a recent study, at 16 weeks of age the obese ZSF1 rats were diabetic, hypertensive, and had renal injury compared to the age-matched lean ZSF1 rats (Hye Khan et al., 2018). Diabetes (plasma glucose >250mg/dL), hypertension (SBP >150mmHg), and proteinuria (>150mg/d) were confirmed in the obese ZSF1 rats. The rats were randomized into four groups (n=6–8/group), Group 1: Lean ZSF1 rats treated with vehicle; Group 2: obese ZSF1 rats treated with vehicle; Group 3: obese ZSF1 rats treated with PTUPB (10mg/kg/d i.p.), and Group 4: obese ZSF1 rats treated with enalapril (10mg/kg/d p.o.). PTUPB administration was carried out using an intra-peritoneal implanted osmotic pump (ALZET® osmotic pump, DURECT Corporation, Cupertino, CA). All rats were weighed, and systolic blood pressure was measured by tail-cuff plethysmography (IITC Life Science Inc., Woodland Hills, CA, USA) during the 8 week treatment protocol. The intra-peritoneal implantation of the osmotic pump under isoflurane (1%) using aseptic procedure. The rats received a single dose (1.5mg/kg) of Buprenorphine SR as analgesic. The rats were monitored for 10 days after surgery for any surgery related complication.

At baseline, intraperitoneal glucose tolerance tests, blood pressure measurements, and urine collections were conducted. At the end of the 8-week treatment protocol blood samples were collected and then rats were euthanized under isoflurane (1%) for plasma and tissue collection. Death was confirmed by bilateral thoracotomy. Urine, blood, plasma, kidney, and liver samples were frozen and stored at −80°C for biochemical assays and other analysis.

The kidney and liver tissue samples were either immersion fixed in 10% neutral buffered formalin for paraffin embedding or processed for frozen section for use in histopathology and immunohistopathological experiments.

Glucose tolerance test

Intra-peritoneal glucose tolerance test was carried out at baseline and at the end of the 8-week treatment protocol. After a fasting blood sample collection, glucose (2 g/kg i.p.) was injected in fasted rats (8–12 hours) followed by tail vein blood sampling at different time points. Blood glucose levels were measured using a glucometer LifeScan (Miltipas, CA, USA).

Biochemical assays

The glycemic status of the rats was determined by measuring hemoglobin A1C (HbA1c) levels in whole blood using a biochemical assay from Crystal Chem and by measuring plasma insulin using ELISA (Mercodia AB, Uppsala, Sweden). Lipid profile was determined by measuring plasma cholesterol, triglyceride, and non-esterified free fatty acid (NEFA) levels using assay kits from Cayman Chemical (Ann Arbor, MI, USA). Plasma low-density lipoprotein (LDL) was measured using a kit from Crystal Chem (Downers Grove, IL, USA). Homeostatic model assessment (HOMA-IR) was carried out to determine insulin sensitivity in experimental groups. As reported earlier, HOMA-IR was calculated from fasting blood glucose (Antunes et al., 2016). Liver enzymes aspartate aminotransferase (AST) and alanine aminotransferase (ALT) were measured using commercial assay kits (Sigma Millipore, St. Louis, MO, USA). Urinary protein and creatinine were measured calorimetrically using assay kits from Cayman Chemical. Urinary levels of albumin and monocyte chemoattractant protein-1 (MCP-1) were determined using ELISAs from Exocell (Philadelphia, PA, USA) and BD Biosciences (San Jose, CA, USA), respectively.

RNA Isolation and Real-Time PCR analysis

Kidney mRNA was isolated from whole kidney homogenate of each individual sample by RNeasy Mini Kit (QIAGEN, CA, USA) according to the manufacturer's protocol. The purity and the amount of mRNA samples were quantified spectrophotometrically. For each sample, 1μg of total RNA was reverse transcribed to cDNA using iScript™ Select cDNA Synthesis Kit (Bio-Rad, Hercules, CA, USA). Real-Time (RT) PCR analysis were carried out using cDNAs to study renal mRNA expressions of TNF-α, IL1β, IL-6, IL-2, and TGF-ß. Gene expression was quantified by iScript One-Step RT-PCR Kit with SYBR green using the MyiQ™ Single Color RT-PCR Detection System (Bio-Rad Laboratories, Hercules, CA, USA). Dissociation curve analysis was done with iQ5 Optical System Software, Version 2.1 (Bio-Rad Laboratories, Hercules, CA, USA. During RT-CR, denaturation was done at 95°C for 2 min followed by 40 cycles at 95°C for 10s and 30s at 60°C. Each sample run in triplicate and fold change in gene expression compared to controls were calculated using comparative threshold cycle (C_t) method. The expression levels of the gene of interest were determined by normalizing C_t values to three housekeeping genes and the final data are expressed as $2^{\Delta\Delta}C_t$. All statistical analyses were carried out using 6–8 samples from each experimental group.

Histopathological analysis

Kidney and liver tissues were fixed in formalin and paraffin embedded. The paraffin embedded tissues were cut into 4μm sections for histological analysis. Tissue sections were deparaffinized, re-hydrated, and kidney tissue slices were stained with Periodic Acid-Schiff (PAS) and Picrosirius Red (PSR). Glomerulosclerosis and mesangial matrix expansion were scored from kidney sections stained with PAS staining using methods described earlier (Hye Khan et al., 2018;2019). Histological analysis was done at a magnification of 400X to assess glomerular injury, and renal tubular proteinaceous cast was assessed at a magnification of 200X using Nikon NIS Elements Software (Nikon Instruments Inc., Melville, NY, USA). The percentage area positive for proteinaceous cast was calculated from the mean of eight cortical and five medullary fields for each animal. Fibrosis in the kidney and liver were determined from kidney and liver sections stained with PSR and examined at a magnification of 200X. In the kidney, the percentage area positive for collagen was calculated as the fibrotic area from the mean of eight cortical and five medullary fields for each kidney sample. The mean percentage of collagen positive liver fibrotic areas were calculated from 20 fields in each liver sample. In assessing liver steatosis, frozen liver sections (10 μm) were stained with Oil Red O dye according to manufacturer's protocol (Abcam, Cambridge, MA, USA). The percent of liver tissue area with lipid accumulation was calculated as described earlier (Kochan et al., 2015). The percentage area positive for lipid accumulation was calculated from the mean of 20 fields (at 200X magnification) for each animal using Nikon NIS Elements Software. Histological scoring was carried out by two observers who were blinded to the identity of the experimental groups.

Immunohistopathological analysis

Immune cell infiltration in the kidney was determined using immunohistopathological analysis. Tissue sections were incubated with rodent declocker solution (Biocare Medical, Concord, CA, USA) at 95°C for antigen retrieval (Hye Khan et al., 2016). Kidney sections were immunostained with anti-CD68 (1:100; Serotec, Raleigh, NC, USA) to determine renal macrophage/monocyte infiltration. Biotinylated rat anti-mouse secondary antibody (1:200) was used for development with avidin-biotinylated HRP complex (Vectastain ABC Elite kit, Vector Laboratories, Burlingame, CA, USA) followed by hematoxylin counterstaining. Stained tissue sections were examined by light microscopy (400x magnification) and digital images were taken for analysis using Nikon NIS Elements Software. Kidney macrophage/monocyte infiltration was determined by counting CD-68 positive cells. As described earlier, (Hye Khan et al., 2016) the number of positive cells per field was divided by the metric area of the field to obtain the number of positive cells per mm^2. All immunohistopathological analysis were done in blinded fashion by two observers and followed the guideline of the British Journal of Pharmacology (Alexander et al., 2018).

Immunofluorescence analysis

Formalin formalin-fixed and paraffin-embedded kidney sections (4μm) were de-paraffinized, re-hydrated, and incubated with rodent declocker solution (Biocare Medical, Concord, CA, USA) at 95°C for antigen retrieval. Kidney sections were then immunostained with anti-nephrin (1:100; Santa Cruz Biotechnology, Inc, Dallas, TX, USA) to determine renal

expression of nephrin. Donkey anti-rabbit IgG H&L (Alexa Fluor® 488) secondary antibody (1:200; Abcam, Cambridge, MA, USA) was used for development with fluorescence quenching liquid (Vector Laboratories, Burlingame, CA, USA). Immunostained sections were examined by Nikon 55i fluorescence with a green excitation (200x magnification) and digital images were taken for analysis using Nikon NIS Elements Software. Nephrin expression in the kidney was determined by measuring the percentage of nephrin positive kidney areas. Two observers blinded to the identity of the samples conducted nephrin image analysis in kidney sections. All experiments and data analysis were carried out according to the guideline of the British Journal of Pharmacology (Alexander et al., 2018).

Determination of glomerular albumin permeability

Glomeruli from 8–10 week Sprague Dawley rats were isolated as previously described (Ilatovskaya, 2015) using a variable-sieving process (150μm, 106μm, then 75μm) after an *in-vivo* renal perfusion of high-molecular weight FITC-labeled dextran (150kD, TdB Consultancy AB, Uppsala, Sweden). Each condition was tested with 3 or more rats, and a minimum of 9 glomeruli. Glomeruli were affixed to the optical window of poly-L-lysine coated culture dish (MatTek, Ashland, MA), and bathed in a 5% BSA solution containing (in mM): 145 NaCl, 2 CaCl2, 4.5 KCl, 2 MgCl2, 10 HEPES, TRITC-labeled dextran, pH 7.35 (adjusted with NaOH). Only de-encapsulated glomeruli with detached afferent and efferent arteriole were included. Using an AR-1 confocal microscope, a Z-stack of 27 images (total thickness of ~72 μm) was collected while in the initial 5% solution (baseline), which was followed by a repeated collected every 2 min following bath exchange to 1% albumin bath solution, for a total of 10 minutes. Glomeruli were either pre-incubated for 5 minutes in angiotensin II (10μM) to induce permeability in the presence and absence of PTUPB (1μM) to determine its effects on permeability. Following the conclusion of the experiment, volumetric recompositing of individual z-planes was carried out using Fiji image processing package (ImageJ 2.0.0, National Institutes of Health, USA) and Origin Pro 6.0 (Origin Lab, Northampton, MA).

Data and Analysis

Statistical analysis was done only for the experiments where n=5 or greater/group. The group size used in each experiment was the number of independent values and the statistical analysis is carried out only on independent values. All outliers are included in statistical analysis and presentation of the data. Data are reported as box and whisker plots with median and minimum to maximum. Figure 4E is plotted as mean ± S.E.M. The statistical significance between two groups was determined by a two-tailed unpaired Student's t test (and among more than two groups it was determined by repeated measure one-way analysis of variance followed by Tukey's post-hoc test) using GraphPad Prism® Version 4.0 software (GraphPad Software Inc, La Jolla, CA, USA). Difference between two groups was considered significant when probability values of P were less or equal to 0.05. This manuscript followed the requirements and recommendation on experimental design and analysis recommended by the British Journal of Pharmacology (Curtis et al., 2018).

RESULTS

PTUPB reduces blood pressure and lacks anti-diabetic actions in obese ZSF1 rats

Obese ZSF1 rats were severely diabetic with 60 to 75% higher fasting blood glucose, increased HbA1c, increased HOMA index, decreased rate of glucose clearance, and marked hyperinsulinemia compared to lean ZSF1 rats (Figure 1). Neither interventional PTUPB nor enalapril treatment attenuated hyperglycemia, hyperinsulinemia, and insulin resistance in obese ZSF1 rats. All markers of overt type 2 diabetes remained markedly elevated compared to lean ZSF1 rats. The obese ZSF1 rats had increased body weight (733±11g) compared to lean ZSF1 rats (470±9g), and neither PTUPB (702±7g) nor enalapril (722±10g) treatments affected body weight of obese ZSF1 rats. Systolic blood pressure was higher in obese ZSF1 rats (182±7 mmHg) compared to lean ZSF1 rats (139±5 mmHg). In obese ZSF1 rats 8-week PTUPB and enalapril treatments reduced blood pressure. Blood pressure averaged 161±9 mmHg in PTUPB and averaged 147±10 mmHg in enalapril treated obese ZSF1 rats.

PTUPB improves plasma lipids in obese ZSF1 rats

Plasma cholesterol, triglycerides, NEFA, and LDL-cholesterol were 70–90% higher in obese ZSF1 rats compared to lean ZSF1 rats. Interventional PTUPB treatment markedly improved the lipid profile of obese ZSF1 rats and reduced plasma lipids to levels similar to lean ZSF1 rats. Interestingly, enalapril treatment did not affect the lipid profile of obese ZSF1 rats and the plasma lipid levels remained elevated in obese ZSF1 rats (Figure 2).

PTUPB reduces renal injury in type 2 diabetic obese ZSF1 rats

Obese ZSF1 rats demonstrated marked renal injury compared to lean ZSF1 rats. In obese ZSF1 rats, albuminuria was more than 40 fold higher compared to lean ZSF1 rats. Obese ZSF1 rats had 4 to14-fold higher renal cortical and medullary cast area compared to lean ZSF1 rats. Interventional PTUPB treatment markedly reduced kidney injury with albuminuria reduced by 40% and tubular cast formation reduced by 60% compared to vehicle obese ZSF1 rats. Enalapril also attenuated kidney injury and exhibited an equipotent effect as PTUPB in attenuating albuminuria, while it was relatively weaker in attenuating renal tubular cast formation in obese ZSF1 rats (Figure 3A–D).

Obese ZSF1 rats demonstrated marked glomerular injury with a glomerular injury score that was 80% higher than lean ZSF1 rats. Both interventional PTUPB and enalapril treatments equipotently attenuated glomerular injury by 50% in obese ZSF1 rats (Figure 4 A, C). Consistent with marked glomerular injury, the obese ZSF1 rats had 60% lower renal nephrin expression compared to lean ZSF1 rats. PTUPB and enalapril treatments equipotently elevated nephrin expression in the kidney of obese ZSF1 rats (Figure 4 B, D). Experiments in isolated glomeruli demonstrate that angiotensin II markedly elevated glomerular albumin permeability. Interestingly, PTUPB directly protected the glomerular filtration barrier and attenuated angiotensin II-induced increase glomerular albumin permeability. In the presence of PTUPB, angiotensin II-induced glomerular albumin permeability was >50% lower than angiotensin II alone (Figure 4E).

Renal fibrosis was 60% higher in obese ZSF1 rats compared to lean ZSF1 rats. Interventional PTUPB and enalapril treatments demonstrated marked anti-fibrotic actions and equipotently reduced renal collagen deposition in obese ZSF1 rats (Figure 5A–C).

In the present study, marked renal inflammation with elevated urinary MCP-1 excretion and infiltration of renal macrophages was evident in obese ZSF1 rats. Urinary MCP-1 excretion was 80% higher in obese ZSF1 rats and PTUPB reduced urinary MCP-1 excretion by 53%. Enalapril also demonstrated anti-inflammatory action in obese ZSF1 rats and reduced MCP-1 excretion by 28%. Moreover, renal inflammation in the obese ZSF1 rats were evident with 10–45 times higher expression of TNF-α, IL1β, IL-6, IL-2, and TGF-ß in the kidney compared to lean ZSF1 rats. PTUPB and enalapril reduced renal expression of these cytokines in obese ZSF1 rats (Figure 6 D). In obese ZSF1 rats, elevated chemokine level was accompanied by marked renal infiltration of immune cells, and obese ZSF1 rat kidneys had 80% higher CD-68 positive immune cells compared to lean ZSF1 rats. PTUPB and enalapril reduced renal infiltration of immune cells in obese ZSF1 rats by 60 and 45%, respectively (Figure 6 A–C). Interestingly, we demonstrated that PTUPB and enalapril acted similarly with PTUPB demonstrating a superior trend in reducing renal injury and inflammation in type 2 diabetic obese ZSF1 rats.

PTUPB reduces liver injury and steatosis in obese ZSF1 rats

Type 2 diabetic obese ZSF1 rats had liver injury along with hyperlipidemia. Obese ZSF1 rats had 2–3 fold higher plasma levels of two important liver injury biomarkers, AST and ALT, compared to lean ZSF1 rats. Interventional PTUPB but not enalapril treatment lowered AST and ALT plasma levels to levels similar to that of lean ZSF1 rats (Figure 7A, B). The obese ZSF1 rats had marked liver fibrosis with a 5-fold higher liver collagen expression compared to lean ZSF1 rats. PTUPB treatment markedly reduced liver collagen expression in the obese ZSF1 rats. Enalapril treatment was ineffective in lowering liver fibrosis in obese ZSF1 rats (Figure 7C, E). The obese ZSF1 rats had marked hepatosteatosis with 3 times higher liver steatotic area compared to lean ZSF1 rats. PTUPB treatment attenuated hepatosteatosis in the obese ZSF1 rats by 50%. Enalapril treatment did not affect hepatosteatosis in obese ZSF1 rats. (Figure 7D, F).

DISCUSSION

Diabetic nephropathy is a major cause of ESRD worldwide. According to the World Health Organization (WHO), 1 in every 11 adults worldwide are diabetic (Saran et al., 2020). This high incidence of diabetes is linked to the high incidence of diabetic nephropathy and consequent ESRD. Approximately 20–40% of all diabetic patients develop diabetic kidney disease in their lifetime, which often progresses to ESRD (Isomaa et al., 2001; Grundy, 2006). Unfortunately, despite the recent progress in our understanding, the complicated pathophysiology of diabetic nephropathy has limited our success to treat and manage diabetic nephropathy. Hence, there is growing interest in developing novel therapies that will target multiple pathophysiological factors of type 2 diabetes and its renal complications (Roche et al., 2015).

Over the years, several studies demonstrated critical etio-pathological roles of eicosanoids in the type 2 diabetes and associated kidney disease (Luo and Wang, 2011; Lorthioir et al. 2012; Molinar-Toribio et al., 2015). Indeed, a large number of studies demonstrated that eicosanoid metabolites are associated with type 2 diabetes, blood pressure, lipid levels, and insulin signaling (Imig, 2018; Bellucci et al., 2017; Nasrallah et al., 2016; Harris, 2008). In the present interventional study, we investigated the effect of a novel molecule, PTUPB, that concurrently acts on two eicosanoid pathways in overt type 2 diabetic obese ZSF1 rats. Initial studies found a higher kidney mRNA expression of sEH and COX-2 in vehicle treated obese ZSF1 rats. PTUPB markedly elevated levels of EETs and reduced levels of pro-inflammatory thromboxane B_2 (TBX_2) and prostaglandin E2 (PGE_2) in the kidney of type 2 diabetic obese ZSF1 rats (Figure S1). PTUPB inhibits sEH and COX-2 enzymes to manipulate epoxyeicosatrienoic acids (EETs) and prostanoids. EETs have potent kidney protective effects in multiple disease conditions (Imig, 2018). However, the EETs are short lived and sEH converts them to their inactive diols. Hence, sEH inhibitors were developed as an effective way in increasing EET levels. Inhibitors of sEH have been demonstrated to be organ protective in multiple disease conditions including cardiometabolic syndrome (Imig, 2012; 2018). Likewise, COX inhibitors, particularly COX-2 inhibitors have cardiovascular and kidney protective effects (Harris, 2013). Inhibition of a specific biosynthetic arachidonic acid pathway could alter the metabolic flux resulting in side effects (Sonnweber et al., 2018). Interactions and changes in metabolic flux have been determined for COX-2 and sEH inhibitors (Kim et al., 2017). PTUPB is a dual acting molecule and that concurrently inhibits sEH and COX-2 resulting in potent kidney protective effects while reducing side effects (Hye Khan et al., 2016, Wang et al., 2018). These previous studies and those of the present study demonstrate that manipulating COX-2 and sEH with PTUPB changes eicosanoid metabolites in a manner that avoids side effects while effectively decreasing diabetic kidney injury.

These finding are consistent with several studies that have shown PTUPB beneficial actions. PTUPB prevents development of diabetic kidney injury in Zucker Diabetic Fatty (ZDF) rat (Hye Khan et al., 2016), suppresses the growth of glioblastomas (Li et al., 2017), and improves sepsis outcomes (Zhang et al., 2020a), and attenuates pulmonary fibrosis (Zhang et al., 2020b). Most importantly, these studies found that PTUPB was superior to sEH or COX-2 inhibitors alone or their combination (Li et al., 2018; Zhang et al., 2014). For instance, a study with mouse xenograft model of bladder cancer found that PTUPB potentiated the anti-cancer activity of cisplatin (Wang et al., 2017). This experimental study also found that PTUPB was superior to the sEH inhibitor t-AUCB and the COX-2 inhibitor celecoxib or their combination (Wang et al., 2017). In the present study, our findings demonstrate that interventional treatment with the dual acting sEH/COX-2 inhibitor, PTUPB, reduces diabetic kidney injury in type 2 diabetic, hypertensive, and hyperlipidemic obese ZSF1 rats.

In type 2 diabetic obese ZSF1 rats, we compared the efficacy of interventional PTUPB treatment with an angiotensin converting enzyme (ACE) inhibitor, enalapril. It is important to note that ACE inhibitors are widely used for blood pressure control and are particularly beneficial in hypertensive type 2 diabetic subjects to treat diabetic nephropathy (Hunsicker, 2004; Batlle et al., 2012). Interestingly, we found that PTUPB did not reduce hyperglycemia

and hyperinsulinemia in obese ZSF1 diabetic rats. This is not entirely consistent with the findings of an earlier study where we reported that PTUPB prevents development of type 2 diabetes in ZDF rats (Hye Khan et al., 2016). The prophylactic PTUPB treatment was given prior to an elevation in fasting blood glucose and insulin resistance to the ZDF rats. Indeed, the objective of that earlier study was to investigate if PTUPB could prevent development of type 2 diabetes. Findings of this previous study prompted us to carry out the present study to investigate the ability of interventional PTUPB treatment to reduce diabetes and its complication in a rat model of severe type 2 diabetes and diabetic nephropathy. Our findings demonstrate that interventional PTUPB treatment failed to reduce blood glucose or improve glucose homeostasis in obese ZSF1 rats. Similar to interventional PTUPB treatment, interventional ACE inhibitor treatment with enalapril did not affect hyperglycemia and insulin resistance in obese ZSF1 rats. These findings are in accord to our earlier findings on the effects of enalapril in obese ZSF1 diabetic rats (Hye Khan et al., 2018). In contrast to our findings, there are studies that demonstrate beneficial enalapril effects on blood glucose and insulin sensitivity. These studies found that enalapril improved insulin sensitivity in fructose-fed spontaneously hypertensive and Cohen Diabetic rats (Vuorinen-Markkola and Yki-Järvinen, 1995). Enalapril is also reported to improve glucose storage and insulin sensitivity in hypertensive type 1 diabetic patients (Rosenthal et al., 1995). The discrepancy between our findings in obese ZSF1 rats and these earlier studies could be due to the different interventional experimental design and the use of different diabetic rat models. Overall, we demonstrate that dual sEH/COX-2 inhibitor PTUPB or enalapril interventional treatment did not reduce type 2 diabetes in obese ZSF1 rats.

An important finding of the present study is the reduction in kidney injury by interventional PTUPB treatment in type 2 diabetic obese ZSF1 rats. The obese ZSF1 rats develop diabetic nephropathy with marked kidney functional and structural injuries (Hye Khan et al., 2018; Bilan et al., 2011; Su et al., 2018). We demonstrate potent renal actions of PTUPB in reducing diabetic nephropathy that is associated with marked renal functional and structural injuries in type 2 diabetic obese ZSF1 rats. The pathophysiology of diabetic nephropathy is complex due to the presence of several comorbid conditions in type 2 diabetic patients. Most often these comorbid conditions are hypertension and hyperlipidemia (Ritz et al., 2001). In clinical studies, it is demonstrated that better blood pressure control in type 2 diabetes decreased the onset or degree of kidney injury and vascular complications (Steigerwalt, 2008). In the present study, interventional PTUPB treatment demonstrated marked anti-hypertensive actions in obese ZSF1 rats. A similar anti-hypertensive action of PTUPB has been reported in an earlier study (Hye Khan et al., 2016). This anti-hypertensive action of PTUPB could be related to the sEH inhibitor activity. The sEH inhibitors are widely reported to be anti-hypertensive, and this effect has been attributed to its ability to increase the ratio of EETs to their less biologically active diols (Imig et al., 2002; Neckář et al., 2012; Wang et al., 2000). Unlike sEH inhibition, COX-2 inhibition is not anti-hypertensive (Zhao et al., 2005; Cheng and Harris, 2004) and COX-2 inhibitors do not affect blood pressure in humans and animals (Bombardier et al., 2000). However, some clinical trials have shown that chronic COX-2 inhibition can induce hypertension in patients (Silverstein et al., 2000). Hence, it is likely that the anti-hypertensive effect of PTUPB in this study is due to sEH inhibitory activity.

In diabetic nephropathy, along with tubular injury, glomerular injury is a pathophysiological hallmark of the kidney injury and dysfunction. We demonstrated that the type 2 diabetic obese ZSF1 rats had marked glomerular injury and damage in the glomerular filtration barrier as assessed from reduced expression of slit diaphragm component nephrin. Interventional PTUPB treatment markedly reduced renal injury in type 2 diabetic obese ZSF1 rats. In the preceding sections we have discussed the diabetic kidney injury treating ability of PTUPB in terms of its beneficial actions on metabolic dysfunctions such as hypertension, hyperlipidemia, and also marked renal inflammation in obese ZSF1 rats. Apart from these approaches, we further investigated renal action of PTUPB in an *in vitro* study using isolated glomeruli. We determined the ability of PTUPB in maintaining glomerular permeability, an important functional feature of glomeruli for their efficient filtration capacity. We demonstrated that PTUPB directly maintains normal glomerular permeability. The findings of this *in vitro* study suggest that the renal injury treating ability of PTUPB in diabetic nephropathy is not only caused by its ability to reduce renal inflammation but also due to its direct effects on the glomerular filtration barrier. Indeed, an important role of endogenous CYP450 metabolites of arachidonic acid in maintaining the glomerular protein permeability barrier has been reported. It has been shown that EETs play an important role in maintaining normal glomerular permeability (Williams et al., 2007). Increased COX-2 expression in podocytes also leads to increased glomerular permeability (Cheng et al., 2007). Thus, PTUPB likely decreases glomerular barrier injury through inhibitory actions on both sEH and COX-2.

Elevated renal inflammation is an important pathophysiological factor of diabetic nephropathy, which contributes to the pathophysiology of tubular and glomerular injuries (Donate-Correa et al., 2020) Indeed, chronic inflammation is a hallmark of metabolic diseases including type 2 diabetes, hypertension, and hyperlipidemia. The severity of renal inflammation and its renal consequence depends on the presence of different metabolic pathologies (Hotamisligil, 2006; Zhang et al., 2017). During metabolic diseases the normal physiological regulatory system is disrupted and initiates a cascade of deleterious inflammatory responses in multiple organs including the kidney (Hotamisligil, 2006; Furman et al., 2019). In type 2 diabetes, infiltration of immune cells and cytokine production occur in the abdominal and peri-renal fat and act as vital source of inflammation in the kidney (Ma et al., 2006). In the present study, we demonstrate marked renal inflammation with renal macrophage infiltration and elevated chemokine production and cytokine expression in the kidney of obese ZSF1 rats. This is consistent with earlier metabolic disease studies that demonstrated renal injury associated with increased renal chemokines and immune cell infiltration (Hye Khan et al., 2014,2018; Imig et al., 2012). Interestingly, interventional PTUPB treatment reduced renal inflammation by reducing renal expression of cytokines, decreasing immune cell infiltration, and reducing chemokine MCP-1 production in type 2 diabetic obese ZSF1 rats.

The anti-inflammatory actions of interventional PTUPB treatment in obese ZSF1 rats most likely a consequence of inhibiting both COX-2 and sEH, as inhibiting each of these pathways has the ability to reduce renal inflammation (Gassler et al., 2001; Bombardier et al., 2000). Renal anti-inflammatory actions for sEH inhibitors have been demonstrated in hypertension and diabetes animal models (Imig and Hammock, 2009).

Global sEH knockout (Ephx2−/−) decreased renal inflammation and macrophage infiltration in deoxycorticosterone acetate high salt (DOCA-salt) hypertension (Manhiani et al., 2009). Moreover, in a renal fibrosis model, sEH inhibition either by gene knockout or pharmacological inhibition provided an antifibrotic action by reducing renal inflammation (Kim et al., 2014,2015). Likewise, COX-2 inhibition has demonstrated anti-inflammatory actions in the kidney. Indeed, several studies demonstrated marked anti-inflammatory actions for COX 2 inhibition in multiple renal pathologies including type 2 diabetes (Honma et al., 2013; Fujihara et L., 2003). In an earlier study, we demonstrated that COX-2 inhibitor rofecoxib reduced renal tubular glomerular injury in type 2 diabetic obese ZDF rats, and the renal action of rofecoxib was associated with its anti-inflammatory effect (Dey et al., 2004). Several recent studies demonstrated marked anti-inflammatory actions of PTUPB in multiple pathological conditions and in multiple organs including the kidney. PTUPB reduced systemic inflammation and reduced liver and kidney injury in mice with sepsis (Zhang et al., 2020a). Certain chemotherapy drugs cause treatment limiting macrophage driven cytokine surge and PTUPB treatment prevented the cytokine surge during chemotherapy (Gartung et al., 2019). Overall, we demonstrate a unique biological action of the dual acting sEH/COX-2 inhibitor PTUPB in treating renal inflammation and injury in a type 2 rat model with established renal dysfunction.

In chronic kidney disease, including diabetic nephropathy, disease progression is associated hyperlipidemia which is a common co-morbid condition of type 2 diabetes (Muntner et al., 2000; Ferro et al., 2018). Important and beneficial renal outcomes of current lipid lowering therapies are known on complications in type 2 diabetes patients (Cases and Coll, 2005; Ferro et al., 2018). In the present study, interventional PTUPB treatment demonstrated an interesting lipid lowering action in type 2 diabetic obese ZSF1 rats. This lipid lowering action of PTUPB can be attributed to its sEH inhibitory activity as the lipid lowering effect of sEH inhibition has been reported in several studies (EnayetAllah et al., 2008; Kourounakis et al., 2002). A polymorphism in the sEH gene (EPHX2) has been reported in humans with marked lipid abnormalities. It is reported that the R287Q variant of sEH is associated with elevated plasma cholesterol and triglycerides in familial hypercholesterolemia (EnayetAllah et al., 2008). Additionally, animal studies in sEH null (EPHX2−/−) mice demonstrated lower plasma total cholesterol levels and lower HMG-CoA reductase activity (EnayetAllah et al., 2008). A similar lipid lowering action has been reported for COX-2 inhibition (Imig et al., 2005). These earlier findings are in accord with our current findings in obese ZSF1 rats and led us to suggest that the marked lipid lowering actions of PTUPB is caused by actions on COX-2 and sEH pathways. Contrary to the actions of PTUPB, interventional enalapril treatment did not cause any beneficial effect on lipid profile of obese ZSF1 rats. As reported in an earlier study, it is possible that 12–24 weeks long enalapril treatment could affect lipid profile in obese ZSF1 rats (Bilan et al., 2011). However, it should be noted that in this previous study enalapril treatment was given prior the development of hyperlipidemia. Moreover, it is not yet known if enalapril or any ACE inhibitor can alleviate established hyperlipidemia in a pre-clinical type 2 diabetic nephropathy model like the obese ZSF1 rat.

Apart of diabetic nephropathy, in type 2 diabetes co-morbid conditions like hyperlipidemia and obesity often contribute to multiple organ injury. Type 2 diabetic patients with co-

morbid hyperlipidemia are at high risk to develop chronic liver disease, particularly non-alcoholic fatty liver disease (NAFLD) (Firneisz et al., 2014; Younossi et al., 2019). In the present study, as well as in an earlier study, we demonstrated that diabetic nephropathy is accompanied by liver dysfunction and steatosis in type 2 diabetic obese ZSF1 rats (Hye Khan et al., 2018). Interestingly, interventional PTUPB but not enalapril treatment markedly reduced liver injury and steatosis in obese ZSF1 rats. Our findings are in accord with an earlier study which reported that the ACE inhibitor enalapril did not treat liver dysfunction and steatosis in obese ZSF1 rats (Bilan et al., 2011). In regard to the multi organ protective actions of PTUPB, a recent study demonstrated liver protective effect of PTUPB. It is shown that PTUPB reduced liver weight, liver lipid content, steatosis, and the liver expression of lipolytic/lipogenic and lipid uptake related genes in a high fat diet induced NAFLD mouse model. PTUPB treatment also arrested liver fibrosis with a decreased collagen deposition and expression of several fibrotic markers including α-smooth muscle action (Sun et al., 2020). It is suggested that the effects of PTUPB on liver dysfunction particularly on hepatostetosis is associated with its lipid lowering and anti-inflammatory actions (Sun et al., 2020). The liver protective actions of PTUPB can also be related to the effect of sEH inhibition on the liver. sEH inhibitors reduced liver steatosis in a high-fat diet induced metabolic disease model (Liu et al., 2012). A strong anti-fibrotic action of sEH inhibitor is also reported in carbon tetrachloride induced cirrhotic hepatitis model (Harris et al., 2015). Activation of COX-2 is reported to be involve in liver injury hence, COX-2 inhibitor will have a beneficial liver protective effect (Horrillo et al., 2007). The pathophysiology of NAFLD, particularly the liver fibrosis involves strong inflammatory components (Carr et al., 2016). Considering potent anti-inflammatory actions of PTUPB in multiple organs including liver, it is likely that the PTUPB anti-inflammatory actions contributed to the decreased liver fibrosis. Indeed, it is reported that PTUPB reduced inflammation in lungs, liver, and kidney in several mouse model of sepsis (Zhang et al., 2020a; Yang et al., 2020). Overall, we demonstrated that the dual acting sEH/COX-2 inhibitor, PTUPB, has promising effects on liver dysfunction that is associated with type 2 diabetes and other similar metabolic disorders.

In summary, we tested a unique dual acting sEH/COX-2 inhibitor, PTUPB that given in an interventional manner is not anti-diabetic but can effectively treat diabetic renal injury and several co-morbid conditions in type 2 diabetes. Interventional PTUPB treatment has multiple actions including decreasing diabetic kidney injury, lowering blood pressure, and reducing hyperlipidemia. We further found that PTUPB has promising effect on type diabetes related liver disease. We believe the small molecule dual acting sEH/COX-2 inhibitor PTUPB has promising drug development potential for diabetic nephropathy and other diabetic complications.

Supplementary Material

Refer to Web version on PubMed Central for supplementary material.

FUNDING

A National Institute of Health (NIH) grant (DK103616) and Dr. Ralph and Marian Falk Medical Research Trust Bank of America, N.A., Trustee grant to JDI.

REFERENCES

Afkarian M, Sachs MC, Kestenbaum B, et al. Kidney disease and increased mortality risk in type 2 diabetes. J Am Soc Nephrol. 2013;24(2):302–308. [PubMed: 23362314]

Antunes LC, Elkfury JL, Jornada MN, Foletto KC, Bertoluci MC. Validation of HOMA-IR in a model of insulin-resistance induced by a high-fat diet in Wistar rats. Arch Endocrinol Metab. 2016;60(2):138–142. [PubMed: 27191048]

Batlle D, Wysocki J, Soler MJ (2012) Angiotensin-converting enzyme 2: enhancing the degradation of angiotensin II as a potential therapy for diabetic nephropathy. Kidney Int 81:520–528. [PubMed: 22113528]

Bellucci PN, González Bagnes MF, Di Girolamo G, González CD. Potential Effects of Nonsteroidal Anti-Inflammatory Drugs in the Prevention and Treatment of Type 2 Diabetes Mellitus. J Pharm Pract. 2017;30(5):549–556.; [PubMed: 27194069]

Bilan VP, Salah EM, Bastacky S et al. (2011) Diabetic nephropathy and long-term treatment effects of rosiglitazone and enalapril in obese ZSF1 rats. J Endocrinol 210:293–308. [PubMed: 21680617]

Bombardier C, Laine L, Reicin A, Shapiro D, Burgos-Vargas R, Davis B, Day R, Ferraz MB, Hawkey CJ, Hochberg MC, Kvien TK, Schnitzer TJ. Comparison of upper gastrointestinal toxicity of rofecoxib and naproxen in patients with rheumatoid arthritis, VIGOR Study Group. N. Engl. J. Med. 343 (2000) 1520–1528. [PubMed: 11087881]

Bugger H, Abel ED. Molecular mechanisms of diabetic cardiomyopathy. Diabetologia, 2014, 57:660–71. [PubMed: 24477973]

Carr RM, Oranu A, Khungar V. Nonalcoholic Fatty Liver Disease: Pathophysiology and Management. Gastroenterol Clin North Am. 2016;45(4):639–652. [PubMed: 27837778]

Cases A, Coll E (2005) Dyslipidemia and the progression of renal disease in chronic renal failure patients. Kidney Int Suppl 99:S87–S93.

Cheng H, Wang S, Jo YI, et al. Overexpression of cyclooxygenase-2 predisposes to podocyte injury. J Am Soc Nephrol. 2007;18(2):551–559. [PubMed: 17202413]

Cheng HF, Harris RC. Cyclooxygenases, the kidney, and hypertension. Hypertension. 43(2004) 525–530. [PubMed: 14732722]

Dey A, Maric C, Kaesemeyer WH, Zaharis CZ, Stewart J, Pollock JS, Imig JD. Rofecoxib decreases renal injury in obese Zucker rats. Clin Sci (Lond) 2004;107(6):561–570. [PubMed: 15307815]

Donate-Correa J, Luis-Rodríguez D, Martín-Núñez E, et al. Inflammatory Targets in Diabetic Nephropathy. J Clin Med. 2020;9(2):458.

EnayetAllah AE, Luria A, Luo B, Tsai H-J, Sura P, Hammock BD, Grant DF. Opposite Regulation of Cholesterol Levels by the Phosphatase and Hydrolase Domains of Soluble Epoxide Hydrolase, J. Bio. Chem. 283 (2008) 36592–36598. [PubMed: 18974052]

Ferro CJ, Mark PB, Kanbay M, et al. Lipid management in patients with chronic kidney disease Nat Rev Nephrol. 2018;14(12):727–749 [PubMed: 30361677]

Firneisz G Non-alcoholic fatty liver disease and type 2 diabetes mellitus: the liver disease of our age?. World J Gastroenterol. 2014;20(27):9072–9089. [PubMed: 25083080]

Fujihara CK, Antunes GR, Mattar AL, et al. Cyclooxygenase-2 (COX-2) inhibition limits abnormal COX-2 expression and progressive injury in the remnant kidney. Kidney Int. 2003;64(6):2172–2181.]. [PubMed: 14633140]

Furman D, Campisi J, Verdin E, et al. Chronic inflammation in the etiology of disease across the life span. Nat Med. 2019;25(12):1822–1832. [PubMed: 31806905]

Gassler N, Elger M, Kränzlin B, Kriz W, Gretz N, Hähnel B, Hosser H, Hartmann I. Podocyte injury underlies the progression of focal segmental glomerulosclerosis in the fa/fa Zucker rat, Kidney Int. 60 (2001) 106–116. [PubMed: 11422742]

Grundy SM (2006) Drug Therapy of the Metabolic Syndrome: Minimizing the Emerging Crisis in Polypharmacy. Nat Rev Drug Discovery 5: 295–309. [PubMed: 16582875]

Harris RC. An update on cyclooxygenase-2 expression and metabolites in the kidney. Curr Opin Nephrol Hypertens. 2008;17(1):64–69. [PubMed: 18090672]

Harris RC. Physiologic and pathophysiologic roles of cyclooxygenase-2 in the kidney. Trans Am Clin Climatol Assoc. 2013;124:139–151. [PubMed: 23874018]

Harris TR, Bettaieb A, Kodani S et al. (2015) Inhibition of soluble epoxide hydrolase attenuates hepatic fibrosis and endoplasmic reticulum stress induced by carbon tetrachloride in mice. Toxicol Appl Pharmacol 286:102–111 [PubMed: 25827057]

Homer BL, Dower K. 41-Week Study of Progressive Diabetic Nephropathy in the ZSF1 fa/fa^{CP} Rat Model. Toxicol Pathol. 2018;46(8):976–977. [PubMed: 30278832]

Honma S, Takahashi N, Shinohara M, et al. Amelioration of cisplatin-induced mouse renal lesions by a cyclooxygenase (COX)-2 selective inhibitor. Eur J Pharmacol. 2013;715(1–3):181–188. [PubMed: 23747596]

Horrillo R, Planagumà A, González-Périz A, et al. Comparative protection against liver inflammation and fibrosis by a selective cyclooxygenase-2 inhibitor and a nonredox-type 5-lipoxygenase inhibitor. J Pharmacol Exp Ther. 2007;323(3):778–786. [PubMed: 17766677]

Hotamisligil GS (2006) Inflammation and metabolic disorders. Nature 444:860–867. [PubMed: 17167474]

Hunsicker LG (2004) Emerging trends for prevention and treatment of diabetic nephropathy: blockade of the RAAS and BP control. J Manag Care Pharm (5 Suppl A):S12–S17.

Hwang SH, Wagner KM, Morisseau C, Liu JY, Dong H, Wecksler AT, Hammock BD. Synthesis and structure-activity relationship studies of urea-containing pyrazoles as dual inhibitors of cyclooxygenase-2 and soluble epoxide hydrolase. J Med Chem. 2011; 54:3037–3050. [PubMed: 21434686]

Hye Khan MA, Hwang SH, Sharma A, Corbett JA, Hammock BD, Imig JD. A dual COX-2/sEH inhibitor improves the metabolic profile and reduces kidney injury in Zucker diabetic fatty rat. Prostaglandins Other Lipid Mediat. 2016;125:40–47. [PubMed: 27432695]

Hye Khan MA, Kolb L, Skibba M, et al. A novel dual PPAR-γ agonist/sEH inhibitor treats diabetic complications in a rat model of type 2 diabetes. Diabetologia. 2018;61(10):2235–2246. [PubMed: 30032428]

Hye Khan MA, Neckář J, Cummens B, Wahl GM, Imig JD (2014) Azilsartan decreases renal and cardiovascular injury in the spontaneously hypertensive obese rat. Cardiovasc Drugs Ther 28:313–322. [PubMed: 24842561]

Hye Khan MA, Schmidt J, Stavniichuk A, Imig JD, Merk D. A dual farnesoid X receptor/soluble epoxide hydrolase modulator treats non-alcoholic steatohepatitis in mice. Biochem Pharmacol. 2019;166:212–221. [PubMed: 31129048]

Ilatovskaya DV, Palygin O, Levchenko V, Endres BT, Staruschenko A. The Role of Angiotensin II in Glomerular Volume Dynamics and Podocyte Calcium Handling. Sci Rep. 2017;7(1):299. [PubMed: 28331185]

Imig JD, Hammock BD. Soluble epoxide hydrolase as a therapeutic target for cardiovascular diseases, Nat. Rev. Drug Discov. 8 (2009) 794–805. [PubMed: 19794443]

Imig JD, Walsh KA, Hye Khan MA et al. (2012) Soluble epoxide hydrolase inhibition and peroxisome proliferator activated receptor γ agonist improve vascular function and decrease renal injury in hypertensive obese rats. Exp Biol Med (Maywood) 237:1402–1412. [PubMed: 23354399]

Imig JD, Zhao X, Capdevila JH, Morisseau C, Hammock BD. Soluble epoxide hydrolase inhibition lowers arterial blood pressure in angiotensin II hypertension, Hypertension. 39(2002) 690–694. [PubMed: 11882632]

Imig JD, Zhao X, Zaharis CZ, Olearczyk JJ, Pollock DM, Newman JW, Kim IH, Watanabe T, Hammock BD. An orally active epoxide hydrolase inhibitor lowers blood pressure and provides renal protection in salt-sensitive hypertension, Hypertension. 46 (2005) 975–981. [PubMed: 16157792]

Imig JD. Epoxides and soluble epoxide hydrolase in cardiovascular physiology. Physiol Rev. 2012; 92(1):101–30. [PubMed: 22298653]

Imig JD. Prospective for cytochrome P450 epoxygenase cardiovascular and renal therapeutics. Pharmacol Ther. 2018;192:1–19. [PubMed: 29964123]

Imig JD. Prospective for cytochrome P450 epoxygenase cardiovascular and renal therapeutics. Pharmacol Ther. 2018;192:1–19. [PubMed: 29964123]

Isomaa B, Almgren P, Tuomi T et al. (2001) Cardiovascular morbidity and mortality associated with the metabolic syndrome. Diabetes Care 24:683–689. [PubMed: 11315831]

Kim HS, Kim SK, Kang KW. Differential Effects of sEH Inhibitors on the Proliferation and Migration of Vascular Smooth Muscle Cells. Int J Mol Sci. 2017; 18.

Kim J, Imig JD, Yang J, Hammock BD, Padanilam BJ. Inhibition of soluble epoxide hydrolase prevents renal interstitial fibrosis and inflammation. Am J Physiol Renal Physiol. 2014;307(8):F971–F980. [PubMed: 25164080]

Kim J, Yoon SP, Toews ML, et al. Pharmacological inhibition of soluble epoxide hydrolase prevents renal interstitial fibrogenesis in obstructive nephropathy. Am J Physiol Renal Physiol. 2015;308(2):F131–F139. [PubMed: 25377915]

Kourounakis AP, Victoratos P, Peroulis N, Stefanou N, Yiangou M, Hadjipetrou L, Kourounakis PN. Experimental hyperlipidemia and the effect of NSAIDs, Exp. Mol. Pathol. 73 (2002) 135–138. [PubMed: 12231215]

Li J, Bertram JF. Review: Endothelial-myofibroblast transition, a new player in diabetic renal fibrosis. Nephrology (Carlton), 2010, 15:507–12. [PubMed: 20649869]

Li J, Zhou Y, Wang H, Gao Y, Li L, Hwang SH, et al. COX-2/sEH dual inhibitor PTUPB suppresses glioblastoma growth by targeting epidermal growth factor receptor and hyaluronan mediated motility receptor. Oncotarget. 2017;8:87353–87363. [PubMed: 29152086]

Liu Y, Dang H, Li D, Pang W, Hammock BD, Zhu Y (2012) Inhibition of Soluble Epoxide Hydrolase Attenuates High-Fat-Diet–Induced Hepatic Steatosis by Reduced Systemic Inflammatory Status in Mice. PLoS ONE 7:e39165. [PubMed: 22720061]

Lorthioir A, Guerrot D, Joannides R, Bellien J. Diabetic CVD--soluble epoxide hydrolase as a target. Cardiovasc Hematol Agents Med Chem. 2012;10(3):212–222. [PubMed: 22632263]

Luo P, Wang MH. Eicosanoids, β-cell function, and diabetes. Prostaglandins Other Lipid Mediat. 2011;95(1–4):1–10. [PubMed: 21757024]

Ma S, Zhu XY, Eirin A et al. (2016) Perirenal fat promotes renal arterial endothelial dysfunction in obese swine 508 through tumor necrosis factor-alpha. J Urol 195:1152–1259 [PubMed: 26417644]

Magee C, Grieve DJ, Watson CJ, Brazil DP. Diabetic Nephropathy: a Tangled Web to Unweave. Cardiovasc Drugs Ther. 2017 Dec;31(5–6):579–592. [PubMed: 28956186]

Manhiani M, Quigley JE, Knight SF, Tasoobshirazi ST, Moore T, Brands MW, Hammock BD, Imig JD. Soluble epoxide hydrolase gene deletion attenuates renal injury and inflammation with DOCA-salt hypertension, Am. J. Physiol. Renal. Physiol. 297 (2009) F740–F748. [PubMed: 19553349]

Molinar-Toribio E, Pérez-Jiménez J, Ramos-Romero S et al. (2015) Effect of n-3 PUFA supplementation at different EPA:DHA ratios on the spontaneously hypertensive obese rat model of the metabolic syndrome. Br J Nutr 113:878–87. [PubMed: 25720761]

Muntner P, Coresh J, Smith JC, Eckfeldt J, Klag MJ (2000) Plasma lipids and risk of developing renal dysfunction: the atherosclerosis risk in communities study. Kidney Int 58:293–30. [PubMed: 10886574]

Nasrallah R, Hassouneh R, Hébert RL. PGE2, Kidney Disease, and Cardiovascular Risk: Beyond Hypertension and Diabetes. J Am Soc Nephrol. 2016;27(3):666–676. [PubMed: 26319242]

Neckář J, Kopkan L, Husková Z, Kolář F, Papoušek F, Kramer HJ, Hwang SH, Hammock BD, Imig JD, Malý J, Netuka I, Ošťádal B, Červenka L. Inhibition of soluble epoxide hydrolase by cis-4-[4-(3-adamantan-1-ylureido)cyclohexyl-oxy]benzoic acid exhibits antihypertensive and cardioprotective actions in transgenic rats with angiotensin II-dependent hypertension, Clin. Sci. (Lond). 122(2012):513–525. [PubMed: 22324471]

Ritz E, Tarng DC. Renal disease in type 2 diabetes. Nephrol Dial Transplant. 2001;16 Suppl 5:11–18 [PubMed: 11509679]

Roche C, Guerrot D, Harouki N et al. (2015) Impact of soluble epoxide hydrolase inhibition on early kidney damage in hyperglycemic overweight mice. Prostaglandins Other Lipid Mediat 120:148–154. [PubMed: 26022136]

Rosenthal T, Erlich Y, Rosenmann E, Grossman E, Cohen A. Enalapril improves glucose tolerance in two rat models: a new hypertensive diabetic strain and a fructose-induced hyperinsulinaemic rat. Clin Exp Pharmacol Physiol Suppl. 1995;22(1):S353–S354. [PubMed: 9072425]

Saran R, Robinson B, Abbott KC, et al. US Renal Data System 2019 Annual Data Report: Epidemiology of Kidney Disease in the United States. Am J Kidney Dis. 2020;75(1 Suppl 1):A6–A7. [PubMed: 31704083]

Silverstein FF, Faich G, Goldstein JL, Simon LS, Pincus T, Whelton A, Makuch R, Eisen G, Agrawal NM, Stenson WF, Burr AM, Zhao WW, Kent JD, Lefkowith JB, Verburg KM, Geis GS. Gastrointestinal toxicity with celecoxib vs nonsteroidal anti- inflammatory drugs for osteoarthritis and rheumatoid arthritis: the CLASS study: A randomized controlled trial. Celecoxib Long-term Arthritis Safety Study, JAMA. 284 (2000) 1247–1255. [PubMed: 10979111]

Sonnweber T, Pizzini A, Nairz M, Weiss G, Tancevski I. Arachidonic Acid Metabolites in Cardiovascular and Metabolic Diseases. Int J Mol Sci. 2018;19(11):3285.

Steigerwalt S (2008) Management of Hypertension in Diabetic Patients With Chronic Kidney Disease. Diabetes Spectrum 21:30–36.

Su Z, Widomski D, Ma J, et al. Longitudinal Changes in Measured Glomerular Filtration Rate, Renal Fibrosis and Biomarkers in a Rat Model of Type 2 Diabetic Nephropathy. Am J Nephrol. 2016;44(5):339–353 [PubMed: 27736813]

Su Z, Widomski D, Nikkel A, et al. Losartan improves renal function and pathology in obese ZSF-1 rats. J Basic Clin Physiol Pharmacol. 2018;29(3):281–290 [PubMed: 29397387]

Sun CC, Zhang CY, Duan JX, et al. PTUPB ameliorates high-fat diet-induced non-alcoholic fatty liver disease via inhibiting NLRP3 inflammasome activation in mice. Biochem Biophys Res Commun. 2020;523(4):1020–1026.). [PubMed: 31973813]

Tesch GH. Diabetic nephropathy - is this an immune disorder? Clin Sci (Lond). 2017 Jul 31;131(16):2183–2199. [PubMed: 28760771]

Tofovic SP, Kost CK Jr, Jackson EK, Bastacky SI (2002) Long-term caffeine consumption exacerbates renal failure in obese, diabetic, ZSF1 (fa-fa(cp)) rats. Kidney Int 61:1433–1444. [PubMed: 11918750]

Toth-Manikowski S, Atta MG. Diabetic Kidney Disease: Pathophysiology and Therapeutic Targets. J Diabetes Res. 2015;2015:697010 [PubMed: 26064987]

Vuorinen-Markkola H, Yki-Järvinen H. Antihypertensive therapy with enalapril improves glucose storage and insulin sensitivity in hypertensive patients with non-insulin-dependent diabetes mellitus. Metabolism. 1995;44(1):85–89. [PubMed: 7854171]

Wang F, Zhang H, Ma AH, Yu W, Zimmermann M, Yang J, et al. COX-2/sEH Dual Inhibitor PTUPB Potentiates the Antitumor Efficacy of Cisplatin. Mol Cancer Ther. 2018;17:474–483. [PubMed: 29284644]

Wang JL, Cheng HF, Shappell S, Harris RC. A selective cyclooxygenase-2 inhibitor decreases proteinuria and retards progressive renal injury in rats, Kidney Int. 57 (2000) 2334–2342. [PubMed: 10844603]

Warren AM, Knudsen ST, Cooper ME. Diabetic nephropathy: an insight into molecular mechanisms and emerging therapies. Expert Opin Ther Targets. 2019;23(7):579–591. [PubMed: 31154867]

Williams JM, Sharma M, Anjaiahh S, Falck JR, Roman RJ. Role of endogenous CYP450 metabolites of arachidonic acid in maintaining the glomerular protein permeability barrier. Am J Physiol Renal Physiol. 2007;293(2):F501–F505. [PubMed: 17507602]

Yang HH, Duan JX, Liu SK, Xiong JB, Guan XX, Zhong WJ, et al. A COX-2/sEH dual inhibitor PTUPB alleviates lipopolysaccharide-induced acute lung injury in mice by inhibiting NLRP3 inflammasome activation. Theranostics. 2020;10(11):4749–4761. [PubMed: 32308747]

Younossi ZM, Henry L. The Impact of Obesity and Type 2 Diabetes on Chronic Liver Disease. Am J Gastroenterol. 2019;114(11):1714–1715.) [PubMed: 31599742]

Zhang CY, Duan JX, Yang HH, Sun CC, Zhong WJ, Tao JH, et al. COX-2/sEH dual inhibitor PTUPB alleviates bleomycin-induced pulmonary fibrosis in mice via inhibiting senescence. FEBS J. 2020;287(8):1666–1680. [PubMed: 31646730]

Zhang G, Panigrahy D, Hwang SH, Yang J, Mahakian LM, Wettersten HI, et al. Dual inhibition of cyclooxygenase-2 and soluble epoxide hydrolase synergistically suppresses primary tumor growth and metastasis. Proc Natl Acad Sci U S A. 2014;111(30):11127–11132. [PubMed: 25024195]

Zhang X, Lerman LO. The metabolic syndrome and chronic kidney disease. Transl Res. 2017;183:14–25. [PubMed: 28025032]

Zhang YF, Sun CC, Duan JX, Yang HH, Zhang CY, Xiong JB, et al. A COX-2/sEH dual inhibitor PTUPB ameliorates cecal ligation and puncture-induced sepsis in mice via anti-inflammation and anti-oxidative stress. Biomed Pharmacother. 2020;126:109907. [PubMed: 32114358]

Zhao X, Dey A, Romanko OP, Stepp DW, Wang HH, Zhou Y, et al. Decreased epoxygenase and increased epoxide hydrolase expression in the mesenteric artery of obese Zucker rats. Am. J. Physiol. Regul. Integr. Comp. Physiol. 2005;288(1):R188–R196. [PubMed: 15345471]

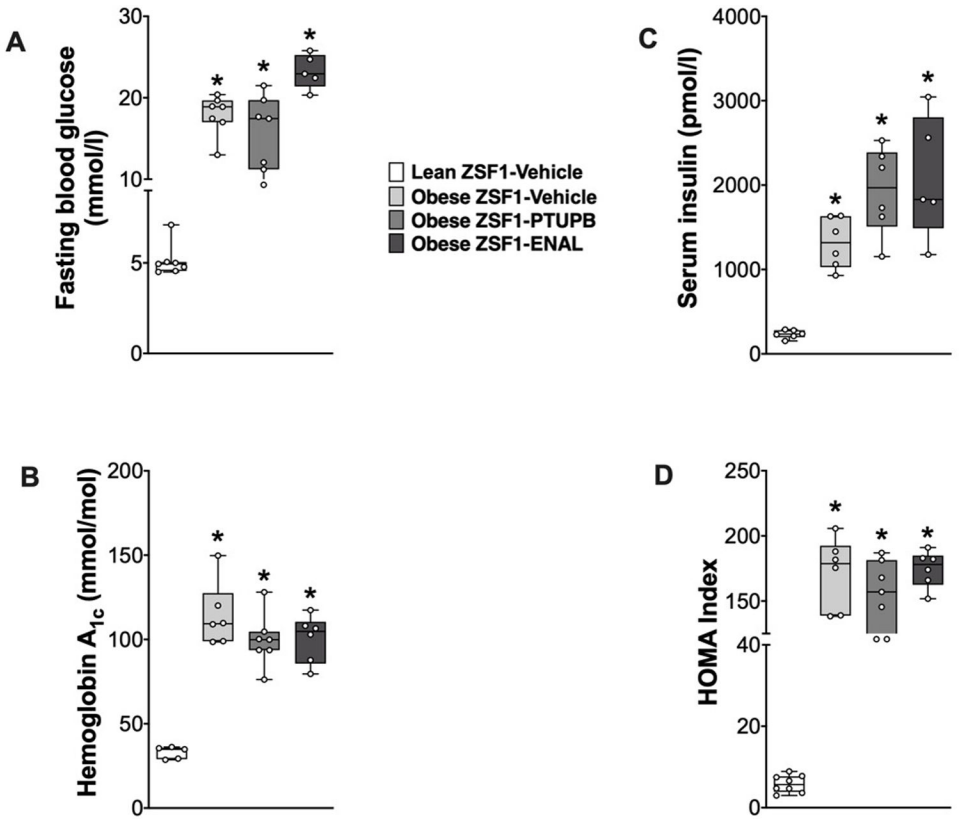

Figure 1: Diabetic parameters in experimental groups.

Fasting blood glucose (A), hemoglobin A_{1c} (B), serum insulin level (C) and HOMA Index at the end of the 8-week experimental protocol. *p<0.05 vs. lean ZSF1-Vehicle; ‡p<0.05 vs. obese ZSF1-Vehicle. ENAL = enalapril. Data are reported as box and whisker plots with median and minimum to maximum, n=6/group.

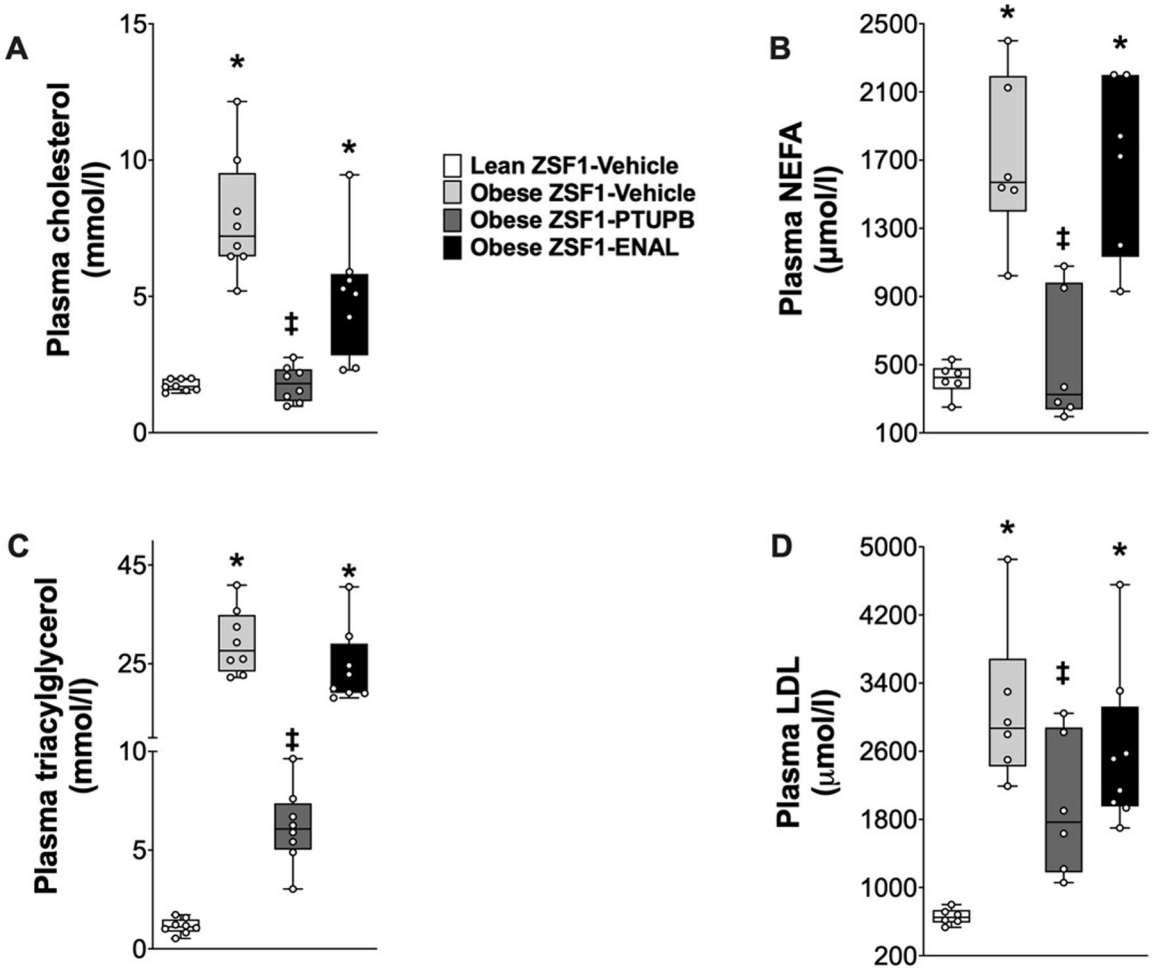

Figure 2: Circulating lipids in experimental groups.

Plasma levels of cholesterol (A), non-esterified free fatty acid (B), triglyceride (C), and LDL-cholesterol (D) at the end of the 8-week experimental protocol. *p<0.05 vs. lean ZSF1-Vehicle; ‡p<0.05 vs. obese ZSF1-Vehicle. ENAL = enalapril. Data are reported as box and whisker plots with median and minimum to maximum, n=6/group.

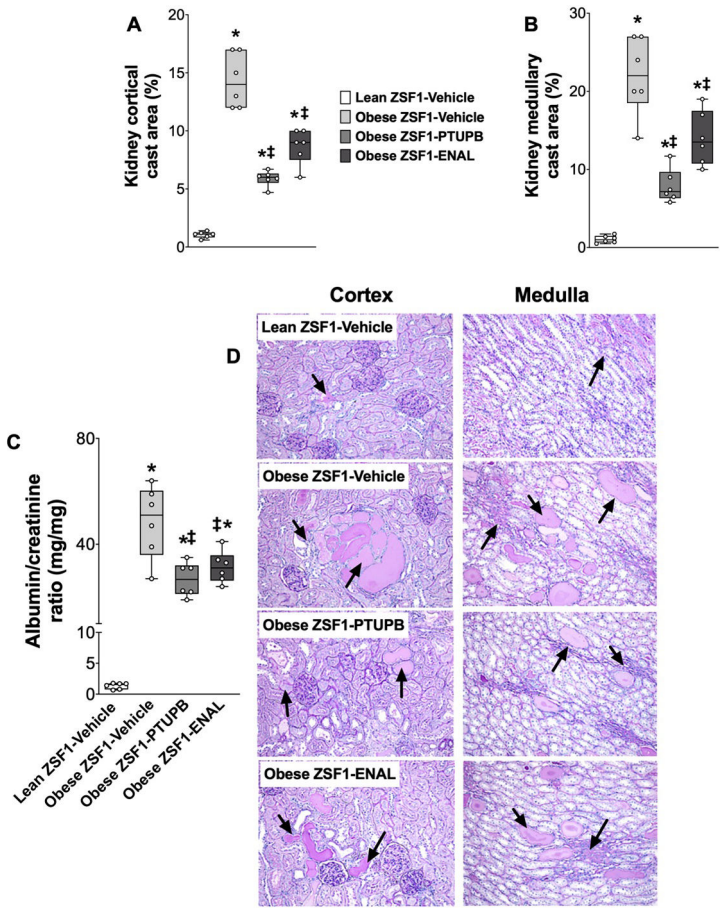

Figure 3: Renal injury in experimental groups.

Calculated values of renal cortical (A) and medullary (B) cast area at the end of the 8-week experimental protocol. Albuminuria (C) and a representative photomicrograph showing tubular cast in the renal cortex and medulla (arrows) of different experimental groups analyzed at the end of the protocol (D). *p<0.05 vs. lean ZSF1-Vehicle; ‡p<0.05 vs. obese ZSF1-Vehicle. ENAL = enalapril. Data are reported as box and whisker plots with median and minimum to maximum, n=6/group.

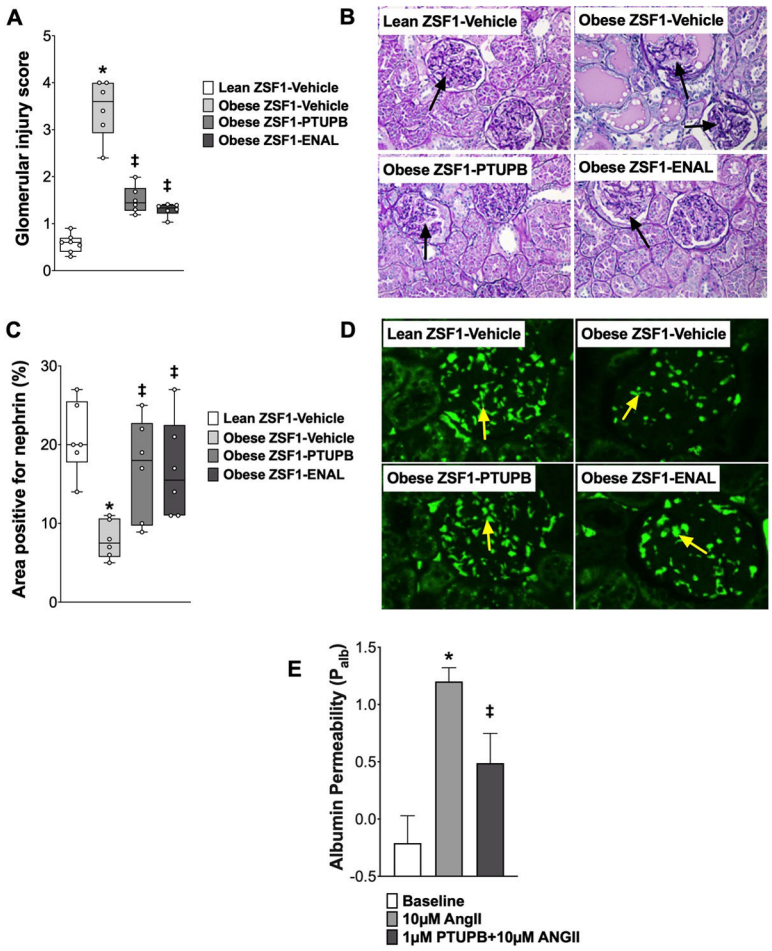

Figure 4: Glomerular injury in experimental groups.

Calculated values of glomerular injury score (A) and glomerular nephrin expression (C) at the end of the 8-week experimental protocol. Representative photomicrograph showing damaged glomeruli (arrows) (B) and nephrin expression (arrows) in the glomeruli of different experimental groups analyzed at the end of the protocol (D). *p<0.05 vs. lean ZSF1-Vehicle; ‡p<0.05 vs. obese ZSF1-Vehicle. ENAL = enalapril. Data are reported as box and whisker plots with median and minimum to maximum, n=6/group. Dual acting sEH-COX-2 inhibitor PTUPB attenuated angiotensin II (ANG II)-induced glomerular albumin permeability (E). *p<0.05 vs. Baseline; ‡p<0.05 vs. ANG II-PTUPB. All data expressed as mean ± SEM, n=10group

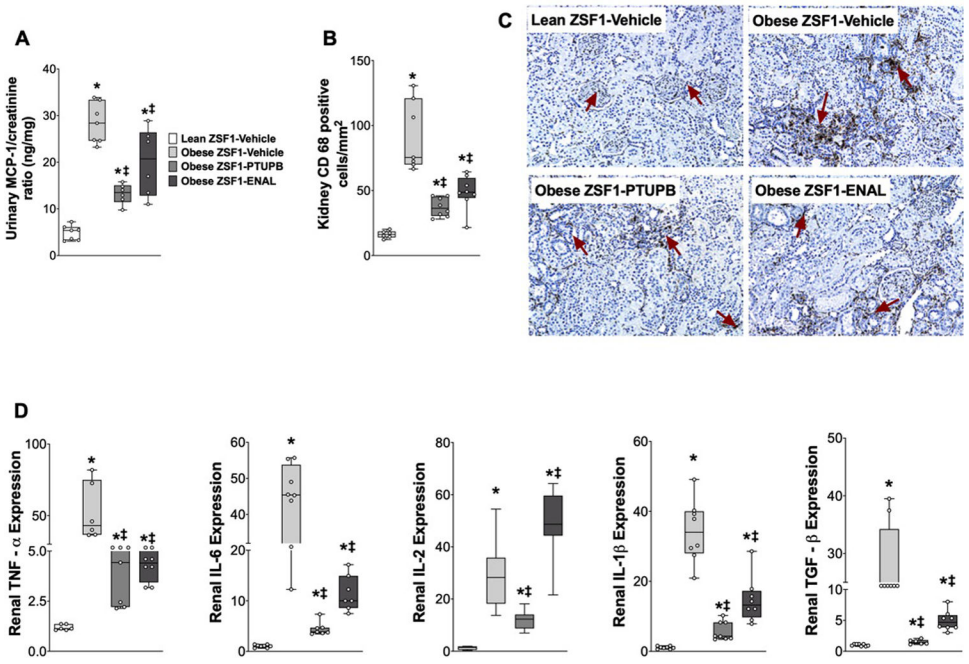

Figure 5: Kidney inflammation in experimental groups.

Urinary excretion of MCP-1 (A), CD-68 positive inflammatory cells in the kidney (B), and representative photomicrograph depicting CD-68 positive cells in the kidney (C) and renal expression of cytokines (D) at the end of the 8-week experimental protocol. *p<0.05 vs. lean ZSF1-Vehicle; ‡p<0.05 vs. obese ZSF1-Vehicle. ENAL = enalapril. Data are reported as box and whisker plots with median and minimum to maximum, n=6/group.

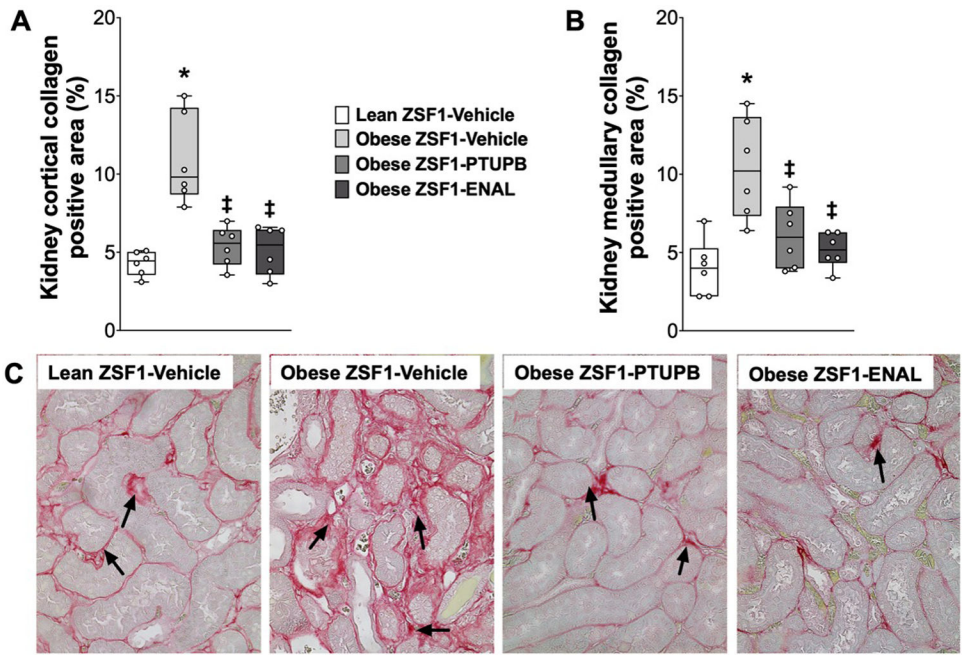

Figure 6: Kidney fibrosis in experimental groups.

Calculated values of renal cortical (A), medullary (B) collagen positive fibrotic area, and a representative photomicrograph showing renal fibrosis (C) at the end of the 8-week experimental protocol. *p<0.05 vs. lean ZSF1-Vehicle; ‡p<0.05 vs. obese ZSF1-Vehicle. ENAL = enalapril. Data are reported as box and whisker plots with median and minimum to maximum, n=6/group.

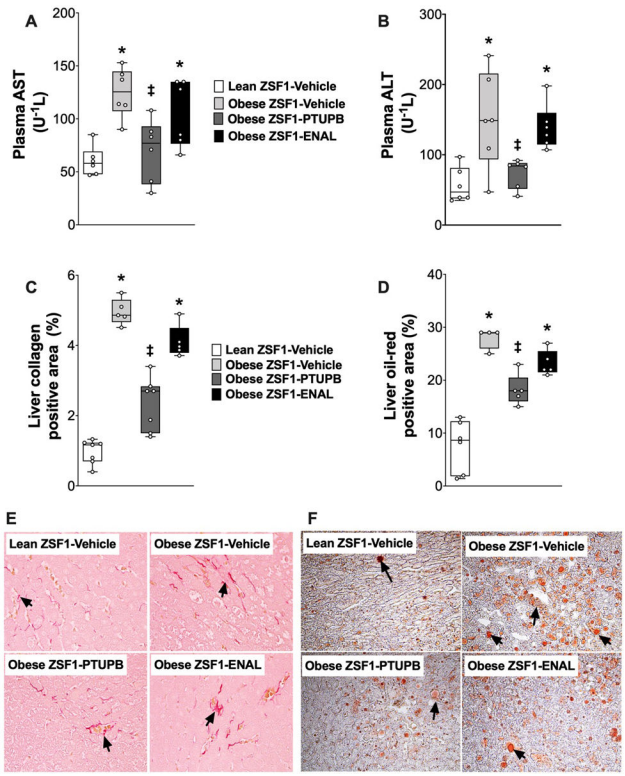

Figure 7: Liver injury in experimental groups.

Plasma levels of AST (A), ALT (B), calculated value of liver collagen positive area (C) and representative photomicrograph depicting collagen positive area (arrows) in the liver (E) at the end of the 8-week experimental protocol. Calculated values of oil o red positive (steatosis) liver area (D) and a representative photomicrograph liver steatosis (arrows) obtained from oil o red staining at the end of the 8-week experimental protocol (F). *p<0.05 vs. lean ZSF1-Vehicle; ‡p<0.05 vs. obese ZSF1-Vehicle. ENAL = enalapril. Data are reported as box and whisker plots with median and minimum to maximum, n=6/group.